Longitudinal Analysis of Ganglion Cell Complex (GCC) Thinning in Glaucomatous Eyes

Jonathan King

UCLA Fielding School of Public Health

BIOSTAT M236: Longitudinal Data

Dr. Robert Weiss

May 23, 2022

Glaucoma is a neurodegenerative eye condition that damages the optic nerve by increasing intraocular pressure and causes loss of cells and nerves in macular structures including the ganglion cell complex (GCC), leading to thinning of the macula. Since macular layer is hypothesized to be directly associated with vision loss, we would expect glaucoma patients to initially have a high rate of GCC thinning within the first year or two, but this rate would decrease once the patient is blind or near-blind and has few macular structures intact. Therefore, the time trend would most likely not be linear but a higher degree polynomial instead. To further explore this trend, exploratory data analysis, fixed effects analysis, and covariance model fitting is conducted. After these analyses, the age covariate is explored to determine if patient age at baseline affects the GCC thickness time trend.

Exploratory data analysis is conducted by constructing a profile plot to observe general trends in the data, performing a correlation analysis to determine how observations at different times are correlated, creating an empirical plot to determine how mean and variance of thickness changes over time, and making an empirical within-subject residual plot to examine within-subject variability. The profile plot reveals that GCC thickness of glaucoma subjects has low fluctuation over time and do not follow a consistent monotonic trend (Figure 1). The data clearly has a random intercept as well as one subject who is a high univariate outlier and quite a few bivariate outliers. Additionally, there is drop out present, with some profiles clearly ending before four years. Correlation analysis using times rounded to the nearest half year reveals significant linear correlations ranging between 0.95 and 1 among observations at all pairs of rounded times (Table 1 and Figure 2). Correlations decrease along rows and are similar for constant lags, making the matrix approximately banded, so the random intercept and slope (RIAS) covariance model should be considered when fitting a model (Table 1). The empirical summary plot constructed using the same rounded times reveals that mean GCC thickness slowly decreases over time from about 83 microns to 78 microns and that variances are approximately equal aside from at the year 4 timepoint, which has a noticeably larger variance that can be attributed to dropout shrinking the sample size (Figure 3). Notably, the average slope does change from negative to positive when rounded time is 1 year but reverts back at 1.5 years. Finally, the empirical within-subject residual plot reveals that most residuals are within 3 microns of their corresponding subject-specific mean while also confirming the presence of the bivariate outliers that are seen in the initial profile plot (Figure 4). This plot also shows the slight downward trend of GCC thickness over time.

Fixed effects analysis of various time trend models using the random intercept (RI) covariance model reveals that the best population time trend is a quadratic time trend because the quadratic time term is significant in the quadratic model (p = .001), but the cubic one is not in the cubic model (p = .09; Table 2). Table 3 shows that after fitting various different random effects covariance models, it can be determined that the random intercept, slope, and quadratic (RIASAQ) covariance model is the most appropriate model for the data based on AIC and BIC using the restricted maximum likelihood (REML) estimation. On average, GCC thickness follows the quadratic model $0.235t^2 - 1.66t + 83.69$, where t is time in years, so the estimated mean rate of GCC thickness change in microns/year at a specific time is approximately given by the linear function $0.47t$ - 1.66 (Table 4). Therefore, as time passes, instantaneous rate of GCC thinning does decrease. Between subjects, the quadratic has an estimated variance of 0.15 microns^2/year^4, and the slope has an estimate variance of 4.63 microns^2/year^2 (Table 5). There is no significant covariance between random intercepts and slopes (p = .09) or quadratics (p = .13), so rates of GCC thinning do not significantly depend on baseline GCC thickness (Table 5).

A profile plot appears to show no difference in the GCC trend over time between subjects younger than 65 years and subjects older than 65 years at baseline (Figure 5), but outliers make the true nature of the relationship unknown. Therefore, the potential effect of the baseline age variable is evaluated using a RIAS covariance model with a population intercept and slope, age main effect, and the interaction between age and the population slope. There is no significant age effect on the GCC thickness intercept or the GCC thickness time trend (Table 6; p = .30), so there is insufficient evidence to conclude that baseline GCC thickness or rate of GCC thickness change over time depends on a subject's baseline age.

Appendix

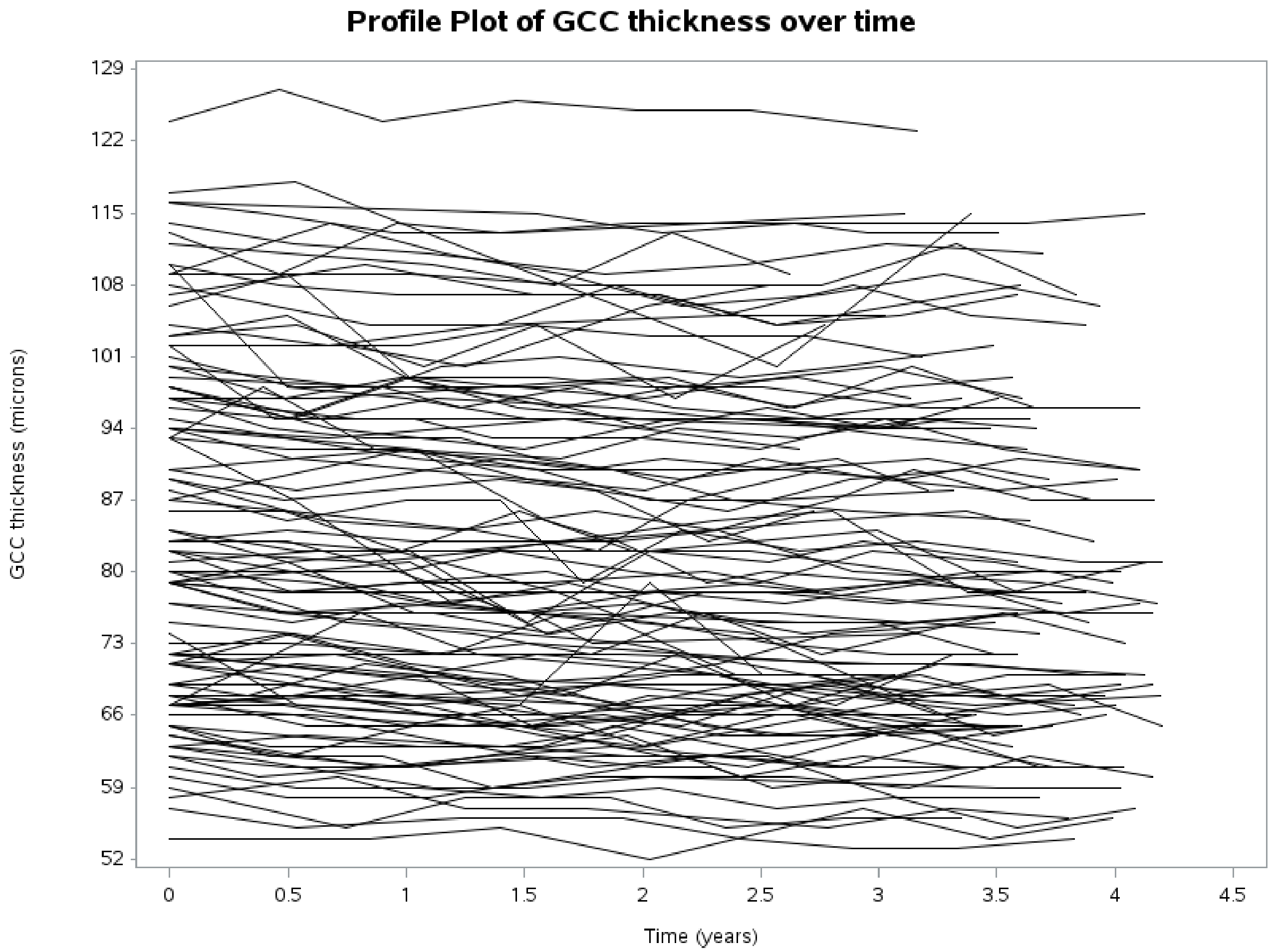

Figure 1. Profile plot of GCC thickness against time. Consecutive observations within the same subject are connected by line segments.

Table 1. Correlation matrix for the macular thickness data. Times are rounded to the nearest half-year and converted to months. Each time in row *j* has a correlation with a time in column *k* from vertical axis, with both *j* and *k* representing indices of the time vector [0, 6, 12, 18, 24, 30, 36, 42, 48], starting from index 1. Each entry includes the correlation between observations at corresponding pairs of times and the calculated *p* value from a hypothesis test against the null hypothesis of no correlation.

	baseline	**month6**	**month12**	**month18**	**month24**	**month30**	**month36**	**month42**	**month48**
baseline	1.000	.989	.982	.978	.972	.972	.963	.967	.957
		<.0001	<.0001	<.0001	<.0001	<.0001	<.0001	<.0001	<.0001
month6	.989	1.000	.989	.981	.977	.971	.968	.964	.952
	<.0001		<.0001	<.0001	<.0001	<.0001	<.0001	<.0001	<.0001
month12	.982	.989	1.000	.990	.987	.984	.980	.977	.963
	<.0001	<.0001		<.0001	<.0001	<.0001	<.0001	<.0001	<.0001
month18	.978	.981	.990	1.000	.987	.987	.983	.982	.973
	<.0001	<.0001	<.0001		<.0001	<.0001	<.0001	<.0001	<.0001
month24	.972	.977	.987	.987	1.000	.991	.986	.983	.980
	<.0001	<.0001	<.0001	<.0001		<.0001	<.0001	<.0001	<.0001
month30	.972	.971	.984	.987	.991	1.000	.992	.981	.978
	<.0001	<.0001	<.0001	<.0001	<.0001		<.0001	<.0001	<.0001
month36	.963	.968	.980	.983	.986	.992	1.000	.990	.989
	<.0001	<.0001	<.0001	<.0001	<.0001	<.0001		<.0001	<.0001
month42	.967	.964	.977	.982	.983	.981	.990	1.000	.994
	<.0001	<.0001	<.0001	<.0001	<.0001	<.0001	<.0001		<.0001
month48	.957	.952	.963	.973	.980	.978	.989	.994	1.000
	<.0001	<.0001	<.0001	<.0001	<.0001	<.0001	<.0001	<.0001	

Scatterplot Matrix

Figure 2. Scatterplot matrix for the macular thickness data. Both horizontal and vertical axes are GCC thickness. Each plot in row *j* has response from time *k* from vertical axis, with both *j* and *k* representing indices of the time vector [0, 6, 12, 18, 24, 30, 36, 42, 48], starting from index 1. Times are rounded to the nearest half-year and converted to months. All subjects with data collected at the times specified by indices *j* and *k* supply one point on the corresponding plot.

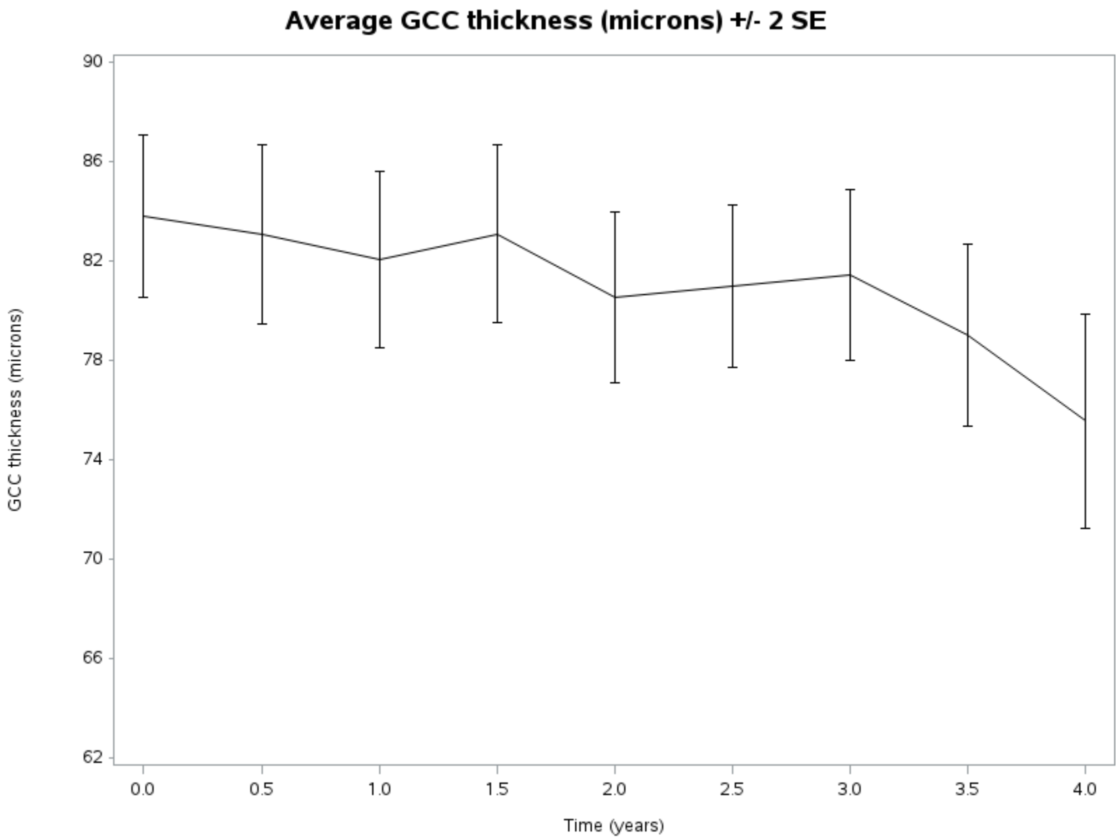

Figure 3. Empirical summary plot of GCC thickness against time. Times are rounded to the nearest half-year. Mean GCC thickness at each timepoint are plotted and connected by life segments. Error bars at each point represent two standard errors in both directions from the mean.

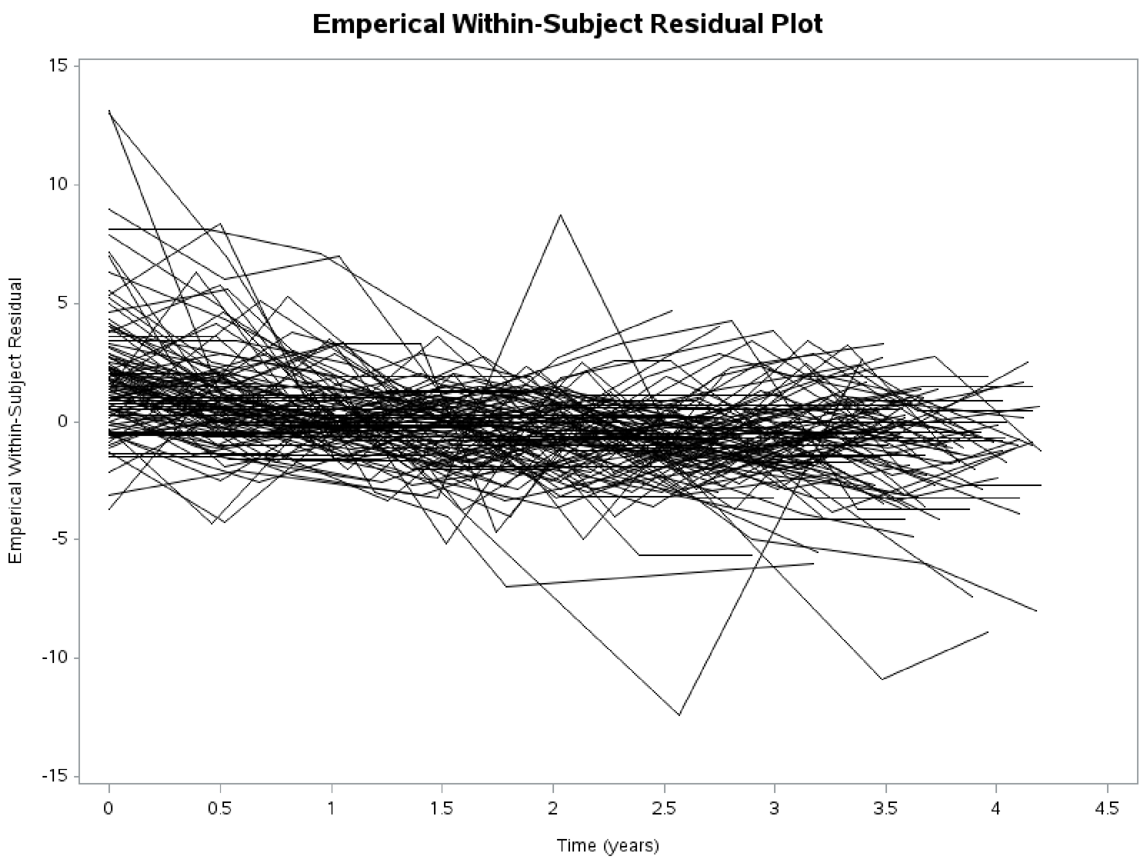

Figure 4. Profile plot of empirical within-subject residuals of GCC thickness against time. Residuals are calculated as the difference between each observation and the subject-specific mean. Consecutive observations within the same subject are connected by line segments.

Table 2. Model output for the linear, quadratic, and cubic models fit using the random intercept (RI) covariance model and the restricted maximum likelihood (REML) estimation. Each row contains a parameter estimate, standard error, and corresponding *t*-statistic and *p*-value from a *t*-test testing the null hypothesis of the parameter estimate equaling 0.

Model	**Parameter**	**Estimate**	**Standard Error**	***t*-statistic**	***p*-value**
Linear	Intercept	83.26	1.61	51.62	<.0001
	Time	-0.79	0.07	-11.26	<.0001
Quadratic	Intercept	83.72	1.62	51.73	<.0001
	Time	-1.66	0.24	-7.02	<.0001
	Time*time	0.23	0.06	3.84	.0001
Cubic	Intercept	83.88	1.62	51.76	<.0001
	Time	-2.45	0.52	-4.73	<.0001
	Time*time	0.78	0.32	2.40	.02
	Time*time*time	-0.09	0.05	-1.71	.09

Table 3. Results of fitting different covariance models using restricted maximum likelihood (REML) estimation. Each row includes the covariance model name, number of covariance parameters, -2 log restricted maximum likelihood, Akaike information criteria (AIC) , and Bayesian information criteria (BIC). AIC and BIC are in "smaller is better" form. Abbreviations: RI = random intercept; RIAS = random intercept and slope; RIASAQ = random intercept, slope, and quadratic; Spatial-POW = spatial power.

Covariance Model	# of Covariance Parameters	REML: -2 Restricted Log Likelihood	AIC (smaller is better)	BIC (smaller is better)
RI	2	4209.34	4213.34	4218.69
RIAS	4	4054.89	4062.89	4073.58
RIASAQ	7	4039.18	4053.18	4071.89
Spatial-POW	2	4090.24	4094.24	4099.58

Table 4. Fixed effect parameter estimates for the selected model (quadratic time trend fit using the random intercept, slope, and quadratic (RIASAQ) covariance model) using restricted maximum likelihood (REML) estimation. Each row contains the parameter estimate, standard error of the estimate, and the corresponding *t*-statistic and *p*-value from a *t*-test testing the null hypothesis of the parameter estimate equaling 0.

Effect	**Estimate**	**Standard Error**	**t-statistic**	***p*-value**
Intercept	83.69	1.64	50.93	<.0001
Time	-1.66	0.28	-5.87	<.0001
Time*time	0.235	0.63	3.69	0.0004

Table 5. Estimated covariance parameters for random intercept, slope and quadratic (RIASAQ) covariance mode using restricted maximum likelihood (REML estimation). Each row includes parameter name/description, parameter estimate, standard error of the estimate and *z*-statistic and *p*-value from a *z*-test against the null hypothesis that the specified parameter is equal to 0.

Covariance Parameter	Estimate	Standard Error	*z*-statistic	*p*-value
Random intercept variance	286.63	39.69	7.22	<.0001
Covariance between random intercepts and slopes	-8.44	4.93	-1.71	.09
Random slope variance	4.63	1.23	3.75	<.0001
Covariance between random intercepts and quadratics	1.68	1.10	1.52	.13
Covariance between random quadratics and slopes	-0.73	0.27	-2.71	.007
Random quadratic variance	0.15	0.063	2.32	.001
Within-subjects variance (Residual)	3.14	0.206	15.27	<.0001

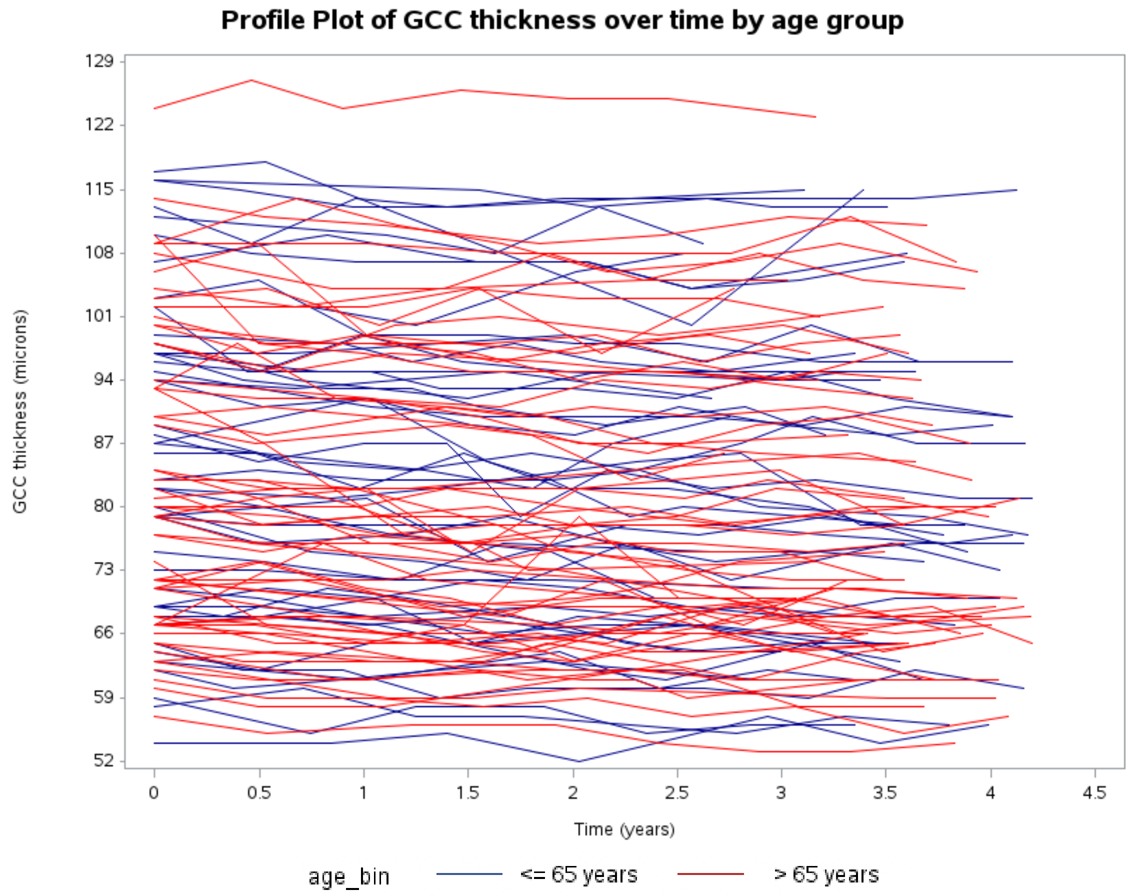

Figure 5. Profile plot of GCC thickness against time for the two age groups. Consecutive observations within same subject are connected by line segments. Subjects aged 65 years or younger have blue profiles; subjects older than 65 years have red profiles.

Table 6. Results of the joint *F*-test testing main effect of baseline age and its interaction with time using the maximum likelihood (ML) estimation. The model used includes a linear time trend fit using a random intercept and slope (RIAS) covariance model. Table includes the tested effect name (age effect), the calculated *F*-statistic, and the corresponding *p*-value.

Effect	***F*-statistic**	***p*-value**
Age effect	1.18	.30